

Development of Proton Computed Tomography for Applications in Proton Therapy

Vladimir Bashkirov¹, Reinhard Schulte¹, George Coutrakon¹, Bela Erdelyi², Kent Wong², Hartmut Sadrozinski³, Scott Penfold⁴, Anatoly Rosenfeld⁴, Scott McAllister⁵, Keith Schubert⁵

¹*Department of Radiation Medicine, Loma Linda University Medical Center, Loma Linda, CA 92354*

²*Department of Physics, Northern Illinois University, DeKalb, IL 60115*

³*Santa Cruz Institute of Particle Physics, University of California Santa Cruz, Santa Cruz, CA 95064*

⁴*Centre for Medical Radiation Physics, University of Wollongong, Wollongong, NSW 2522, Australia*

⁵*Department of Computer Science and Engineering, California State University San Bernardino, San Bernardino, CA 92407*

Abstract. Determination of the Bragg peak position in proton therapy requires accurate knowledge of the electron density and ratio of effective atomic number and mass (Z/A) of the body tissues traversed. While the Z/A ratio is fairly constant for human tissues, the density of tissues varies significantly. One possibility to obtain accurate electron density information of tissues is to use protons of sufficient energy to penetrate the patient and measure their energy loss. From these transmission measurements, it is possible to reconstruct a three-dimensional map of electron densities using algebraic techniques. The interest in proton computed tomography (pCT) has considerably increased in recent years due to the more common use of proton accelerators for cancer treatment world-wide and a modern design concept based on current high-energy physics technology has been suggested. This contribution gives a status update on the pCT project carried out by the pCT Collaboration, a group of institutions sharing interest and expertise in the development of pCT. We will present updated imaging data obtained with a small pCT prototype developed in collaboration with the Santa Cruz Institute of Particle Physics and installed on the proton research beam line at Loma Linda University Medical Center. We will discuss hardware decisions regarding the next-generation pCT scanner, which will permit scanning of head-sized objects. Progress has also been made in the formulation of the most likely path of protons through an object and parallelizable iterative reconstruction algorithms that can be implemented on general-purpose commodity graphics processing units. Finally, we will present simulation studies for utilizing pCT technology for on-line proton dose verification and tumor imaging with positron emission tomography (PET).

Keywords: proton therapy, tomography, imaging, reconstruction.

PACS: 87.57.-s, 87.57.Gg, 87.58Fg, 87.59Fm

INTRODUCTION

Proton computer tomography (pCT) exploration started over three decades ago as an alternative to diagnostic x-ray computer tomography (x-ray CT). From the start, experimental and Monte Carlo studies of pCT performance (1-3) revealed certain advantages versus x-ray CT, namely higher accuracy of electron density reconstruction and lower dose at the same density resolution. On the other hand, it was found that the image quality of pCT is limited by energy loss straggling and multiple Coulomb scattering. But the main drawback was the requirement of a dedicated proton accelerator and beam transport system which made diagnostic pCT scanners substantially more

expensive than x-ray CT scanners and prevented commercial availability of pCT. In recent years, however, interest in pCT arose due to worldwide rapid development of proton and ion treatment centers. The pCT exploration shifted from a diagnostic modality to applications in proton treatment planning and image-guided therapy, where proven pCT benefits such as favorable dose-density resolution and linear stopping power dependence on electron density can be fully exploited utilizing existing accelerators and beam delivery (gantry) systems (4), and where x-ray CT scanners are in use at present. Moreover, image reconstruction software development based on the algebraic reconstruction technique (ART) combined with most likely path (MLP) concept (5,6)

demonstrated that pCT spatial resolution matching that of common CT and MRI scanners is achievable (7). Further, progress in particle detector development allows to design next-generation pCT scanners (8), which can be permanently installed directly in proton (or heavy ion) treatment rooms and utilized for proton (or heavy ion) treatment planning, patient positioning and on-line verification of treatment delivery.

This paper reports on the results obtained with the pCT scanner prototype in a cone-beam set-up at Loma Linda University Medical Center (LLUMC) proton accelerator research beam line. The hardware decisions regarding the next-generation pCT scanner, which will permit scanning of head-sized objects, is also described. Lastly, a GEANT4 simulation of the pCT scanner performance for on-line PET-image-guided proton therapy is presented.

PROTON CONE BEAM SET-UP AND DATA TAKING

As was shown in our previous work (7), the location of proton tracks within phantoms up to 20cm diameter can be determined to a precision of better than 0.5mm on average using external silicon (Si) telescopes, which provide information on proton entrance and exit coordinates and directions. At present, the LLUMC research beam line is equipped with only one Si micro-strip telescope consisting of two tracking modules, each capable of measuring proton hit coordinates and energy deposition in two single-sided Si detectors (0.4mm thick, $64 \times 64 \text{mm}^2$) (9). A possibility of pCT image reconstruction utilizing just one Si telescope, proton residual energy detector, and proton cone beam was studied with a GEANT4-based Monte Carlo simulation and 3D-image reconstruction based on the MLP concept (10).

The result showed that spatial resolution better than 0.1mm can be achieved using one upstream and one downstream 2D-tracking module in a cone beam configuration (Fig. 1) imaging a 4cm diameter phantom (Fig. 2).

In this configuration, coordinates of the well-defined cone beam vertex together with coordinates measured with the upstream tracking module can be used to evaluate entrance position and direction, while the unknown exit direction is estimated from the known entry position and exit coordinates measured with the downstream tracking module. Although reduced accuracy in determination of the exit angle may lead to some artifacts in the reconstructed image, and energy straggling in the scattering foil and collimator walls may reduce the density resolution, this simplified prototype proved useful for first experimental performance studies.

The simulation results were verified with the experimental pCT set-up installed at the LLUMC proton accelerator research beam line. A brass collimator with a 2mm-diameter hole was aligned with the beam axis at the beam exit window and a scattering lead foil of 0.25mm thickness covered the brass collimator exit hole. The tracking telescope was placed on the beam axis 1.5m downstream from the lead foil and the distance between the telescope modules was set to 45mm to accommodate the 40mm diameter phantom in-between the modules. The proton residual energy detector, located behind the telescope, was specially designed for this experiment. It consisted of a rectangular scintillating crystal machined of 40 mm thick CsI(Tl) to stop up to 115MeV protons, with a $64 \times 64 \text{mm}^2$ squared face matching the sensitive area of the tracker. The crystal was viewed by a Hamamatsu S3584-08 photodiode with a $28 \times 28 \text{mm}^2$ sensitive area through an acrylic

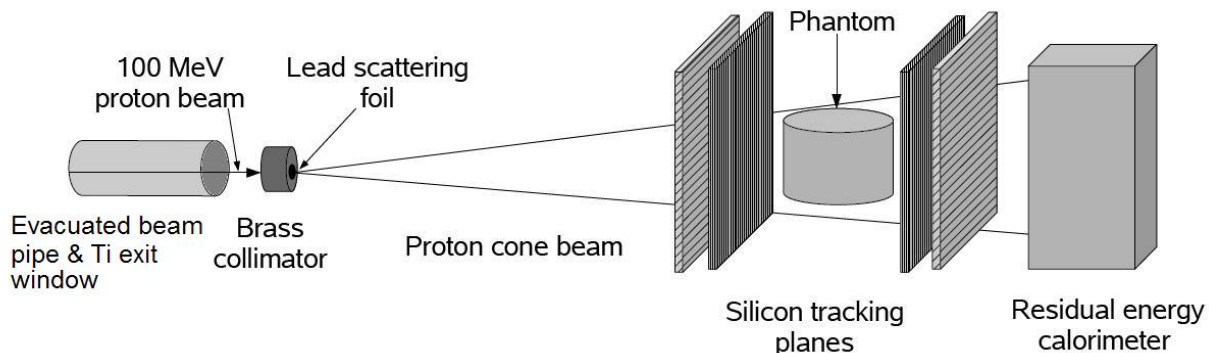


FIGURE 1. Proton cone beam set-up layout. A proton pencil beam collimated with a 2mm-diameter brass collimator is scattered on a 0.25mm thick lead foil to form a cone-like divergent beam. Micro-strip detector modules, each equipped with two single-sided Si detectors, are installed upstream and downstream of the phantom. A CsI:Tl scintillator is used to measure residual proton rest energy.

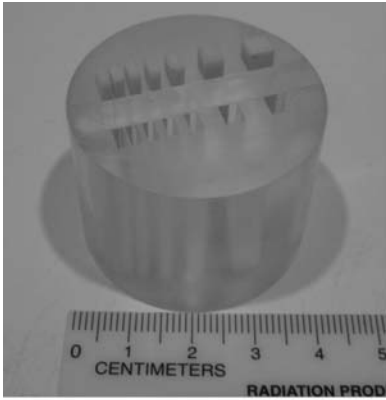


FIGURE 2. Acrylic phantom. The upper row is filled with bone-equivalent plastic, the lower row is empty.

light guide. The light guide and crystal sides were wrapped with Teflon tape, and the crystal face was covered with an aluminized Mylar foil. The detector energy response was evaluated with mono-energetic proton beams. The energy resolution at 100MeV was found to be about 0.5%.

For imaging, we used a cylindrical acrylic spatial resolution phantom, 30mm in height and 40mm in diameter. Two rows of rectangular wells, 25mm in depth and 4 mm in height, were machined in the cylinder (see Fig. 2). The wells had a width and spacing varying from 1 to 4mm. One well row was filled with a bone-equivalent plastic, while the other row was left empty. The phantom was installed on top of an acrylic post mounted on a motorized rotational stage in-between tracking modules (Fig. 3).

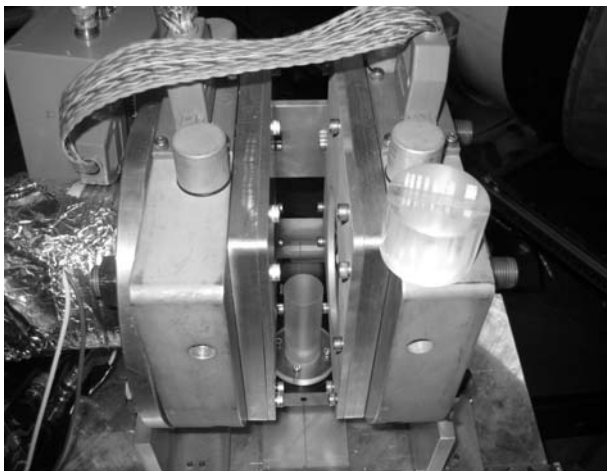


FIGURE 3. Phantom installation.

The phantom was irradiated with a 100MeV proton cone beam at 90 projection angles in increments of 4°.

About 200k events were collected per projection. For each event the following six values were recorded:

- proton energy at phantom entrance calculated as a difference between most probable proton energy after scattering foil and energy deposited in the upstream tracking module;
- proton exit energy calculated as a sum of energy deposited in the downstream tracking module and energy measured by the proton energy detector;
- four track coordinates registered by silicon multi-strip detectors.

EXPERIMENTAL RESULT AND COMPARISON TO MC

The recorded experimental data and similar data set generated by the GEANT4-based Monte Carlo (MC) code simulating the experimental set-up were treated by 3D image reconstruction software exploiting ART combined with the MLP concept given in the Appendix of (11). Reconstruction results presented as the transversal cuts of the 3D image of the phantom are shown in Fig. 4.

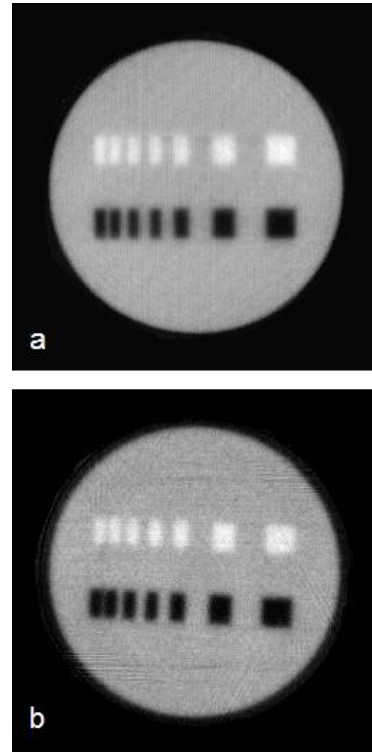


FIGURE 4. Transversal cuts of the 3D phantom image reconstructed from (a) simulated and (b) experimental data.

CONCLUSION AND FUTURE PLANS

We have tested an experimental pCT scanner prototype and reconstructed a small phantom with ART and the most likely path concept. Despite the restricted track reconstruction capability of the present experimental set-up, the reconstruction results demonstrate that a pCT scanner suitable for high-quality image-guided proton therapy is a feasible technical possibility.

At present, we are constructing a full-scale pCT prototype with four Si detector planes and a multi-crystal energy detector large enough to cover the 3D volume of a head phantom. Each Si detector plane is designed as a single printed circuit board holding four 9cm x 9cm silicon strip detectors (SSD), two on each side. The front-side SSDs have the strips oriented in the horizontal direction, the backside SSDs in the vertical direction. The detector readout electronics utilizes ASICs developed at SCIPP for GLAST mission (12). Design of matching multi-crystal energy detector and its readout is in progress.

The availability of such a detector system installed on a clinical proton gantry will also allow us to test new concepts of pCT scanner utilization for on-line verification of target location relative to the beam position. This will be done by using the pCT system to measure the distribution of positron emitting radio-nuclides activated by the treatment proton beam. Preliminary results of a GEANT4 MC simulation show that the proposed pCT system will be able to record approximately 0.4 511 keV γ counts per second when 1Gy of 100 MeV proton dose is delivered to 1mL of soft tissue. Only C^{11} , N^{13} and O^{15} decay channels were considered in this study, thus higher count rates may be observed when the less dominant channels are also included.

Successful implementation of these imaging modalities that become available with a pCT scanner would create a universal device for *in situ* hadron therapy planning, monitoring, and image guidance.

REFERENCES

1. R. H. Huesman, A. H. Rosenfeld, and F. T. Solmitz, "Comparison of heavy charged particles and x-rays for axial tomographic scanning," Report LBL-3040, Lawrence Berkeley Laboratory, 1975.
2. A. M. Cormack and A. M. Koehler, *Phys. Med. Biol.* **21**, 560-569 (1976).
3. K. M. Hanson, J. N. Bradbury, T. M. Cannon, R. L. Hutson, D. B. Laubacher, R. J. Macek, M. A. Paciotti, and C. A. Taylor, *Phys. Med. Biol.* **26**, 965-983 (1981).
4. H. F.-W. Sadrozinski, V. Bashkirov, M. Bruzzi, L. R. Johnson, B. Keeney, G. Ross, R. W. Schulte, A. Seiden, K. Shahnazi, D. C. Williams, and L. Zhang, *Nucl. Instr. and Meth. A* **511**, 275-281 (2003).
5. T. Li, Z. Liang, J. V. Singanallur, T. J. Satogata, D. C. Williams, and R. W. Schulte, *Med. Phys.* **33**, 699-706 (2006).
6. Z. Liang, T. Li, R. Schulte, T. Satogata, D. Williams, and H. Sadrozinski, "Proton Computed Tomography," in *Cancer Imaging, Volume 2: Instrumentation and Applications*, edited by M. A. Hayat, Burlington, MA, Elsevier Academic Press, 2007, pp. 3-16.
7. M. Bruzzi, N. Blumenkrantz, J. Feldt, J. Heimann, H. F.-W. Sadrozinski, A. Seiden, D. C. Williams, V. Bashkirov, R. Schulte, D. Menichelli, M. Scaringella, G. A. P. Cirrone, G. Cuttone, N. Randazzo, V. Sipala, and D. L. Presti, *IEEE Trans. Nucl. Sci.* **54**, 140-145 (2007).
8. R. Schulte, V. Bashkirov, T. Li, J. Z. Liang, K. Mueller, J. Heimann, L. Johnson, B. Keeney, H. F.-W. Sadrozinski, A. Seiden, D. C. Williams, L. Zhang, Z. Li, S. Peggs, T. Satogata, and C. Woody, *IEEE Trans. Nucl. Sci.* **51**, 866-872 (2004).
9. B. Keeney, V. Bashkirov, R. P. Johnson, W. Kroeger, H. Oyama, H. F. Sadrozinski, R. W. Schulte, A. Seiden, and P. Spradlin, *IEEE Trans. Nucl. Sci.* **49**, 1724-1727 (2002).
10. S. N. Penfold, R. W. Schulte, V. Bashkirov, and A. B. Rosenfeld, "Comparison of proton tracking detector configurations for a prototype proton computed tomography system: a simulation study" Conference Record HT6-2 of IEEE Nuclear Science Symposium and Medical Imaging Conference 7, CD-ROM (IEEE Publication), 2007.
11. R. W. Schulte, S. N. Penfold, J. T. Tafas, and K. E. Schubert, *Med. Phys.* **35**, 4849-4856 (2008).
12. H. F.-W. Sadrozinski, *Nucl. Instr. and Meth. A* **466**, 292-299 (2001).